147

DYNAMIC FAILURE: MECHANICAL AND MICROSTRUCTURAL ASPECTS

Marc André Meyers
Department of Applied Mechanics and Engineering Sciences
University of California, San Diego
La Jolla, California 92093-0411

Proc. EURODYMAT
INVITED LECTURE
In press, Oxford, J. Harding, ed.
1994.

$1 + \varepsilon_r + \varepsilon_\sigma = 0.6$
$2\varepsilon_r = -0.4$

Résumé: La rupture dynamique peut être divisée en trois classes: rupture par traction, par compression, et par cisaillement. Les principaux phénomènes impliqués dans la rupture dynamique sont identifiés et les modèles mécaniques qui les incorporent sont présentés. La rupture dynamique en métaux ductiles procède par la germination, croissance et coalescence de vides. Dans les matériaux fragiles, elle se processe par la germination, croissance, et coalescence de fissures. Dans la rupture par cisaillement, la formation de bandes de cisaillement joue un rôle essentiel, et leur évolution est décrite pour un nombre de matériaux. Les éléments microstructurels, qui ont un effet sur la formation et propagation de bandes de cisaillement sont énumerés; ils sont les précurseurs de rupture par cisaillement et traction. La rupture par compression est décrite pour des céramiques et des matériaux géologiques. Les effets de taille de grain, transformations de phase, traitements termiques, précipités et dispersions, porosité, et microfissures sur la rupture dynamique sont présentés.

Abstract: Dynamic failure can be divided into three classes: failure in tension, in compression, and in shear. The principal physical phenomena involved in dynamic failure are identified, and the mechanical models which incorporate them are reviewed. Dynamic failure of ductile metals in tension takes place by the nucleation, growth, and coalescence of voids. For brittle materials, it takes place by the nucleation, growth, and coalescence of cracks. In dynamic failure by shear, adiabatic shear bands play a key role, and their evolution in a number of materials is reviewed. Microstructural elements affect both the initiation and propagation of shear bands, which are precursors to shear and tensile failure. Compressive failure is very important in brittle materials and occurs by the activation of existing flaws in the microstructure. Compressive failure in rocks and ceramics is described. The effects of grain size, phase transformations, heat treatments, second-phase particles, porosity and existing flaws on dynamic failure are discussed.

1. INTRODUCTION

Failure can be defined as the separation of a body into two or more parts; separation requires tension. In this sense, tensile stresses are important for the production of failure. As the rate at which materials are deformed increases, the following effects play an increasingly important role:

a) Mass inertia: this leads to the propagation of elastic, plastic, and shock waves.
b) Thermal inertia: the thermal diffusion distance decreases as the time for deformation decreases, leading to pronounced temperature inhomogenities within the material.
c) Thermal activation and viscosity: the response of dislocations (the primary carriers of plastic

deformation) to applied tractions is determined by their ability to overcome obstacles; at higher propagation velocities phonon and electron viscosity may determine the response. This behavior translates itself into a temperature and strain-rate dependence of flow stress, that is named, in macromechanical terms, as "thermoviscosity".

These three effects determine the elastic, plastic, and failure response of materials.
The infinite complexity of the morphological characteristics of failure can be rationalized by the interplay of the above-named effects (mass inertia, thermal inertia, thermal activation and viscosity) with microstructural characteristics of materials. Prominent among the latter are:

bonding: metallic covalent, ionic
microstructure: grain size, grain-boundary structure, phase transformations, heat treatment effects, compositional effects, etc
structure: crystalline, amorphous, quasicrystalline, polymeric, etc.
mesostructure: biomimetics ;hierarchical structures; composites; synergistic systems.

Dynamic failures can be classified into three groups:

a) tensile failure the state of stress and the dynamics of generation, propagation, and interconnection of flaws dictates the morphology. Under uniaxial strain conditions, this failure is called "spalling".

b) compressive failure: under compressive traction localized regions of tension can be generated in the microstructure, which give rise to failure. Although pure FCC metals (gold, silver, etc.) are mostly immune to this type of failure, less ductile metals (eg., tungsten, steel), ceramics, composites are subjected to this type of failure.

c) shear failure; shear localization, which can have microstructural or thermal origins, often leads to failures. It should be emphasized that the adiabatic shear band is the precursor event, and that it provides a path for crack propagation (fragilized or softened material) which is a tensile stress phenomenon.

In this paper, the microstructural aspects of these three types of failure will be discussed, and a few of the mechanical models that have been developed are briefly presented. The subject matter is very broad, and this author addresses the aspects in greater depth and breadth in a forthcoming book [1]. It is an impossible task to properly review t his extensive field, to which so many outstanding scientists have made contributions , in a few pages. The number of the references in the thousands. A number of books and monographs have recently appeared or are in production, and this complements the early books by Rinehart and Pearson [2], Kolsky [3], Goldsmith [4], and Johnson [5]. Essential advanced texts are Freund [6], Asay and Shahinpoor [7], Davison, Grady, and Shahinpoor [8], Akmadeyev [9], Bai and Dodd [10], Bushman et al [11], Graham [12], and Zukas [13]; as well as the monograph by Curran et al [14]. The author and coauthors (Aimone [15] and Zurek [16]) have two review articles on spalling and dynamic fracture, respectively.

2. DYNAMIC FAILURE IN TENSION

2.1 Mechanical Modeling

Dynamic failure in tension involves high-velocity crack propagation in brittle materials and rapid void growth in ductile materials. Between a spherical void, for a perfectly ductile material, and an infinitely sharp crack tip, for a brittle material, one can envisage an entire range of phenomena. The limiting velocity of a crack in a brittle material has been calculated by Mott [17], at an elementary level, and more completely by Yoffe [18], Broberg [19], Craggs [20], Baker [21], Achenbach [22], and Freund [23-28]. These different studies are varying boundary conditions and crack sizes. Only the results of Freund's work will be illustrated here. Figure 1(c) shows the configuration calculated by Freund [23]: a semi-infinite crack growing at a velocity v (constant) under a time-independent loading σ_{∞}, in an elastic material. The solution involves integral equations, the Laplace transform, and the Wiener-Hopf technique, originally developed for electromagnetic

waves. The stress intensity factor at a velocity v, $K_I(v, t)$ is related to the stress intensity factor at rest, $K_I(0, t)$ by:

$$\frac{K_I(v, t)}{K_I(0, t)} = \frac{1 - \frac{v}{C_R}}{1 - \frac{v}{2C_R}}$$

where C_R is the Rayleigh wave velocity. Figure 1(b) shows the results for two values of the Poisson ratio ν. The stress-intensity factor drops to zero when $v = C_R$. Thus, the Rayleigh wave velocity is the limiting crack velocity. This should be considered as an upper bound, and real materials are subjected to a series of complicating effects that decrease the maximum velocity:

i - plastic deformation at crack tip, increasing work required for crack propagation.

ii - grain boundaries and other barriers and crack-tip deflectors.

iii - crack bifurcation at high velocities predicted from the calculations of Yoffé [18] because of the shifting of the maximum principal stress orientation with increasing velocity. Yoffé [18] predicted a shift in orientation with possible bifurcation at $0.5\ C_S < v < 0.8\ C_S$, where C_S is the shear-wave-velocity, while Congleton [29] and Sih [30] suggested a value of $0.7\ C_R$. Yoffé attributed the bifurcation of cracks to the compression of the stress field ahead of the crak at high velocities and to the generation of maximum principal tensile stress planes away from the plane of the crack. Ravi-Chandar and Knauss [31] conducted careful experiments which suggest another mechanism for the bifurcation of cracks. The interactions of microcracks in the process zone ahead of a major crack are responsible for bifurcation, according to them.

It is possible, in a unique loading situation, to produce supersonic crack propagation, and this was accomplished by Winkler et al [32] by laser irradiation of KCl crystals. A plasma, driven down the crack opening, can produce velocities between 10^4 and 10^5 m/s.

The growth of voids involves considerable plastic deformation, and quasi-static void growth models have been developed by McClintock [33,34] and Rice and Tracey [35], among others. Additional efforts by Glennie [36], Rice and Johnson [37], and McMeeking [38] are also noteworthy.

Curran, Seaman, and Shockey [14] developed the physically-based model involving the nucleation, growth and coalescence of voids in a region undergoing tensile stresses (NAG model). Their approach involves the following expressions for the rate of nucleation, $\dot{N}$, and the rate of growth, $\dot{R}$, of flaws:

$$\dot{N} = \dot{N}_0 \exp\left[(\sigma - \sigma_{r0})/\sigma_1\right]$$

$$\dot{R} = \left(\frac{\sigma - \sigma_{g0}}{4\eta}\right) R$$

σ_{r0} is the tensile threshold stress, $\dot{N}_0$ is the threshold nucleation rate, σ_1 is the stress sensitivity for nucleation, σ_{g0} is the tensile stress threshold for void growth, η is the crack tip viscosity, and R is the crack/void radius.

The yield surface for a material containing voids was modeled by Gurson [39] as:

$$\frac{3}{2}\underline{\sigma}' : \underline{\sigma}' = \left[1 + \phi^2 - 2\phi \cosh\left(\frac{3P}{2\sigma_y}\right)\right] \sigma_y^2$$

ϕ is the volume fraction of pores, $\underline{\sigma}'$ the stress deviator, σ_y the yield stress of the material, and P the hydrostatic stress (tensile or compressive). When $\phi = 0$, it reduces itself to a J_2 flow criterion. Fyfe [40] used the Gurson model to predict dynamic failure by tension in metals.

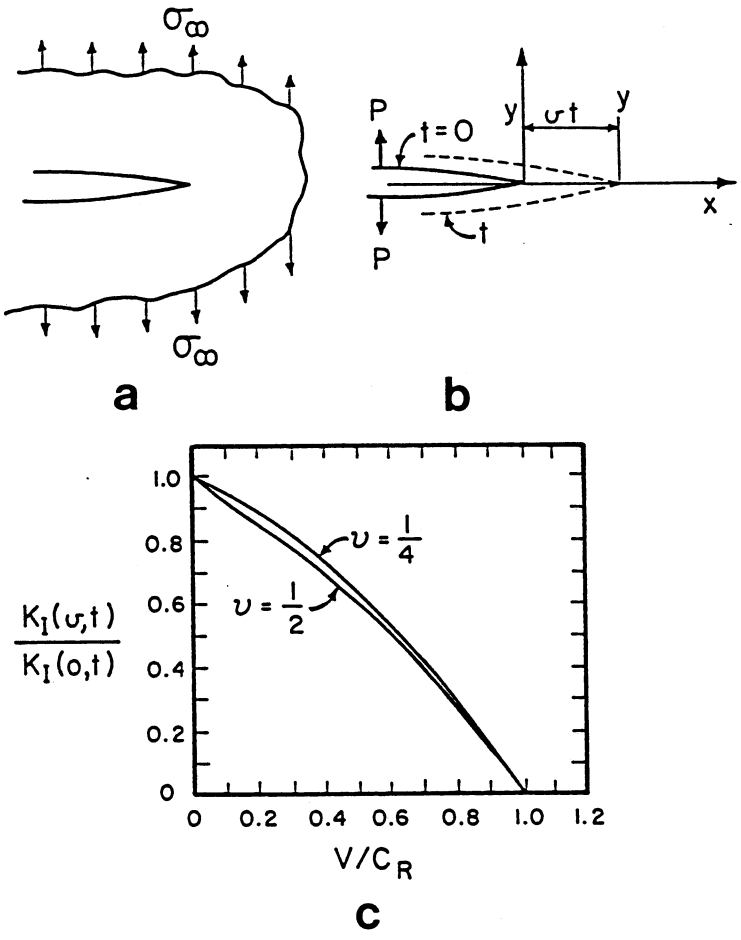

Figure 1. (a) Loading boundary conditions and (b) referential translation in Freund's dynamic crack propagation analysis; (c) normalized stress intensity factor as a function of normalized crack velocity (C_R is Rayleigh speed) (from L. B. Freund [23], Fig. 2).

Johnson [41], based on the Carroll-Holt [42] model, developed an analytical treatment for failure under tension and compared his predictions with spalling experiments in copper.

The treatments discussed above deal with individual cracks or voids. When the collective behavior of cracks is considered, different approaches have to be implemented . In spalling, a continuum model was developed by Davison and Stevens[43].. A damage parameter D was defined, varying from 0 (initial undamaged material) to 1 (final spalled material). This damage parameter was analytically expressed as a function of material parameters. For the case of fragmentation produced by tensile stresses, the early theory of Mott [44] was followed by the Grady-Kipp [45] and Grady [46] approaches, that led to the determination of fragment size as a function of strain rate. Bai, Ke, and coworkers [47-49] have developed a statistical model of microcrack generation, extension, and interconnection.

Louro and Meyers [50, 51], based on observations in alumina, developed a model for the prediction of the fragment size in a specimen subjected to sequential compressive and tensile loading. The compressional portion of the loading pulse (and this will be discussed in Section 4) activate flaws and created cracks which then grow at high velocities during the tensile portion of the pulse. Figure 2 shows the four different stages of fragmentation. Existing flaws (a) are activated by compression,m and new flaws are generated (b). Upon tensile loading, the flaws will grow at velocities dictated by the crack dynamics equations (c). These cracks intersect each other (d) forming fragments. Each growing crack generates an unloaded region (hatched in Fig. 2 (e)) in which no subsequent flaw

activation takes place. A simplified analysis was developed by Louro and Meyers [51]. The crack velocity, V_C, was assumed to be limited by the Rayleigh wave velocity, C_r, as:

$$V_C = C_R\left[1 - e^{\alpha\left(K_I^2 - K_{IC}^2\right)}\right]$$

K_{IC} and K_I are the critical and current values of the stress intensity factor, respectively. By considering flaws that were critical at the onset of tension, N_i, and flaws that were activated during tension, $\dot{N}_V$, Louro and Meyers[51] developed general experience for the crack surface per unit volume as a function of time, stress, and microstructure. The nucleation rate, $\dot{N}_V$, was corrected continuously for the unloaded volume created by the growing cracks.

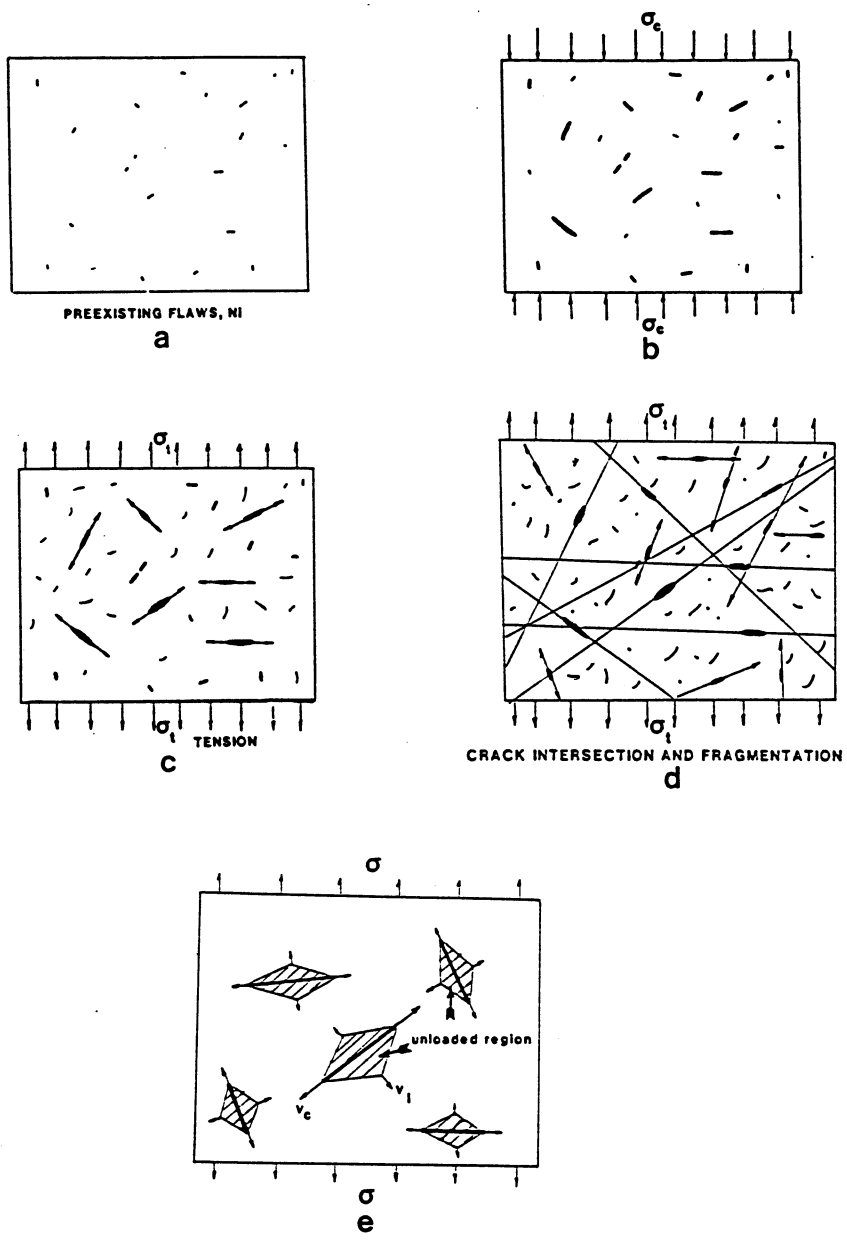

Figure 2. Different stages in fragmentation of brittle material due to stress-wave loading; (a) initial, preexisting flaws; (b) compressive loading and stable growth of flaws; (c) tensile loading; (d) growth of cracks and intersection of free surfaces; (e) unloading of regions surrounding crack growth.

2.2 Microstructural Aspects

The microstructural aspects of dynamic fracture by spalling are extensively discussed by Meyers and Aimone [15] and Zurek and Meyers [16] , among others. The response of materials is complex and is dictated by the existing microstructure and its evolution during shock loading and/or in high-strain rate loading. A wide variety of effects occur, and some of them will be illustrated in this section. We will first review brittle materials, and then ductile materials. A very important aspect of damage is the level at which we are observing it; this level can be, somewhat arbitrarily, classified into microscale, mesoscale, and macroscale. Roughly, these scales correspond to observations as follows:

microscale: scanning and transmission electron microscopy
mesoscale: optical microscopy
macroscale: naked eye.

One phenomenon of great importance is the dependence of fragment size (for a brittle material) on the strain rate. Results by Field and coworkers [52] are shown in Figure 3 for a ceramic impacted at different velocities: 35.6, 46, 76.2, 97.4, and 138 m/s. As the impact velocity is increased, the fragment number increases. A simple Hertzian cone is produced at 35.6 m/s, whereas fine comminution results from the 138 m/s impact. These results are in accord with the Grady-Kipp [45], Grady [46], and Louro-Meyers [50,51] formulations, as well as a significant amount of additional experimental results. Figure 4 shows the formation of microcracks in alumina dynamically loaded in tension. In Figure 4(a) the cracks gave rise to the microcracks, whereas in Figure 4(b) these microcracks were formed at the grain boundaries and are marked by arrows. These results by Louro and Meyers [53] are consistent with experimental observations by Longy and Cagnoux [54] as well as Coscullela et al [55,56]. Figure 5 shows the effect of microstructural parameters, such as grain size, on dynamic fracture of alumina. Under identical loading conditions [53], alumina with a grain size of 24 μm exhibited less macrocracking than alumina with a grain size of 4 μm. The interpretation given by Louro and Meyers[53] to this effect is that these were fewer grain boundaries in the 24 μm alumina; the grain boundaries (Fig. 4(b)) are sources of cracks.

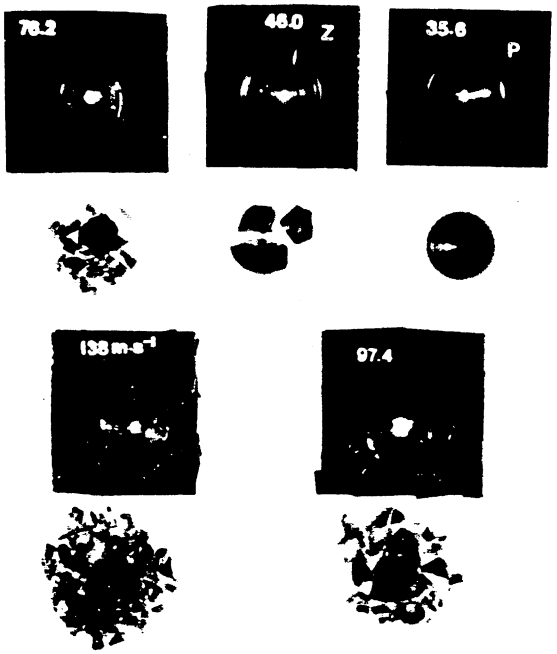

Figure 3. Formation of ejection cone and fragmentation due to impact of glass by spherical projectile at different velocities (marked in m/s). (from J. Field [52], Fig. 21).

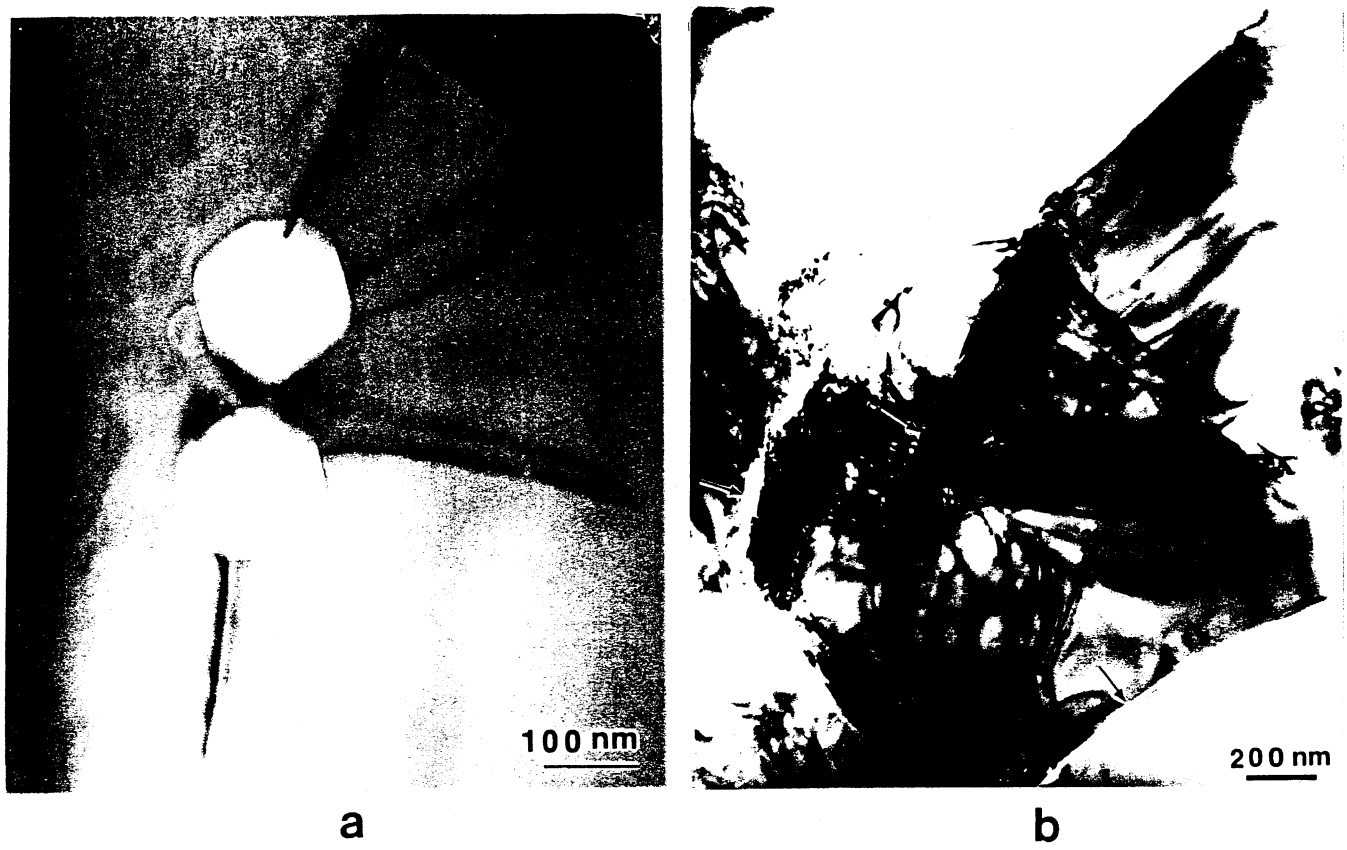

Figure 4. Flaws generated in Al_2O_3 subjected to dynamic tension; (a) cracks at voids; (b) cracks at grain boundaries.

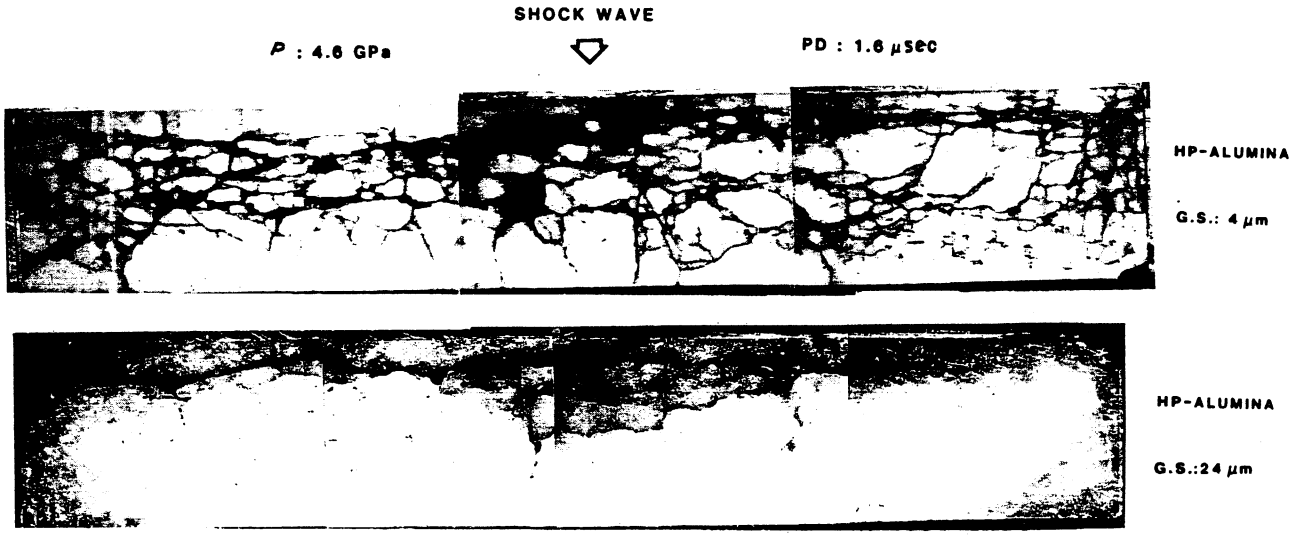

Figure 5. Cross-sections of Al_2O_3 disks impacted by flyer plate technique encapsulated in Al containers; P = 4.6GPa; pulse duration = 1.6μs. (From Louro and Meyers [53]).

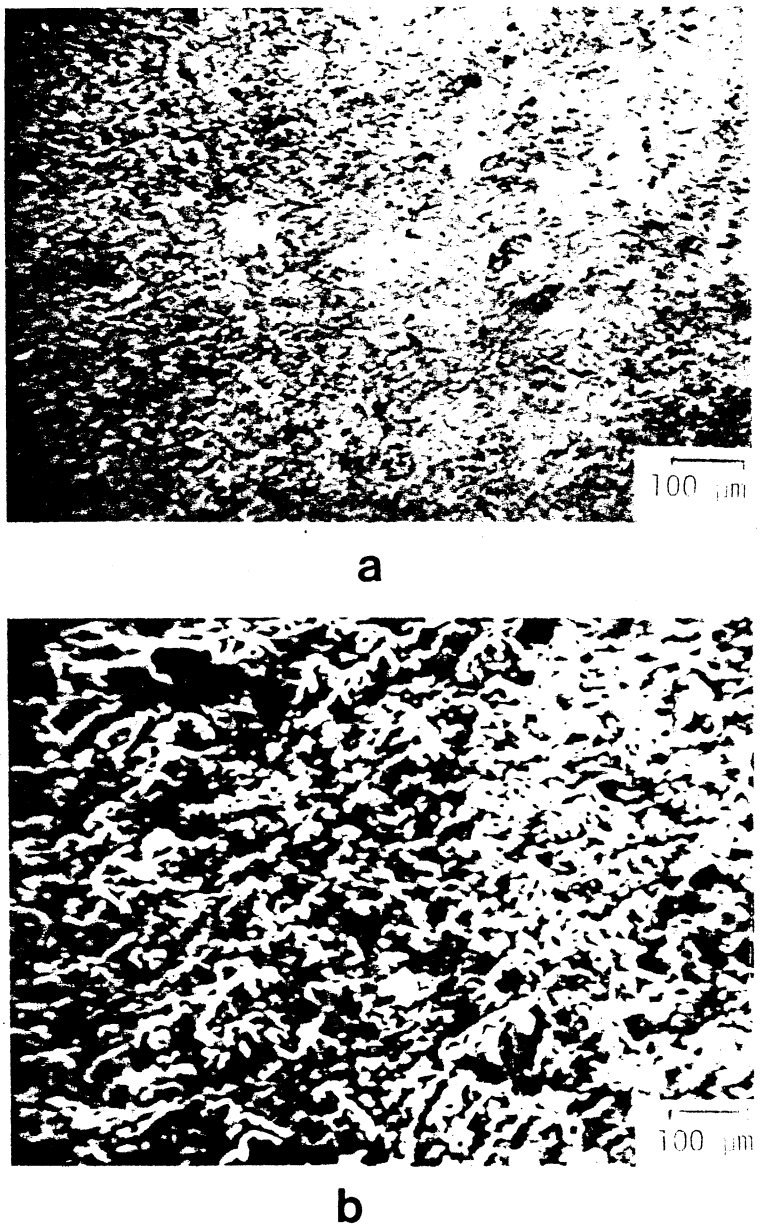

Figure 6 Scanning electron micrographs of spall surfaces in steel; (a) smooth spall; (b) rough spall (From Meyers and Aimone [15]).

In metals one can have both brittle and ductile fracture under tension and the transition from ductile to brittle behavior in steels is dictated both by temperature and strain rate. This response is rooted in dislocation dynamics, as described by Meyers[1]. This transition has a very significant effect on the high-strain-rate fracture of steels, which occurs at a lower stress intensity factor than low-strain-rate fracture. The analysis by Follansbee and Zurek[57] addresses this effect. Another phenomenon of great importance in steels is the drastic change of morphology that occurs when shock pressure (which precedes spalling) exceeds 13 GPa. When this occurs, the spall morphology changes drastically. This phenomenon was first observed by Ivanov and Novikov[58]. Figure 6 shows low-magnification scanning electron micrographs of smooth (P>13 GPa; (a)) and rough (P<13 GPa; (b)) spalls. Upon visual observation, the smooth spall appears as flat as a machined surface. A higher magnification observation of these two morphologies is shown in Figure 7 for an AISI 4340 steel. The fracture produced at 10 GPa is brittle. The fracture produced above the 13 GPa threshold is ductile. The explanation provided by Zurek et al[59] for this phenomenon is that the pre-shocking of the material to P>13 GPa generates a large concentration of defects which can then nucleate cracks upon being subjected to the tensile pulse. The shift from brittle to ductile reponse in steels can be produced by a decrease in grain size, an analogous response.

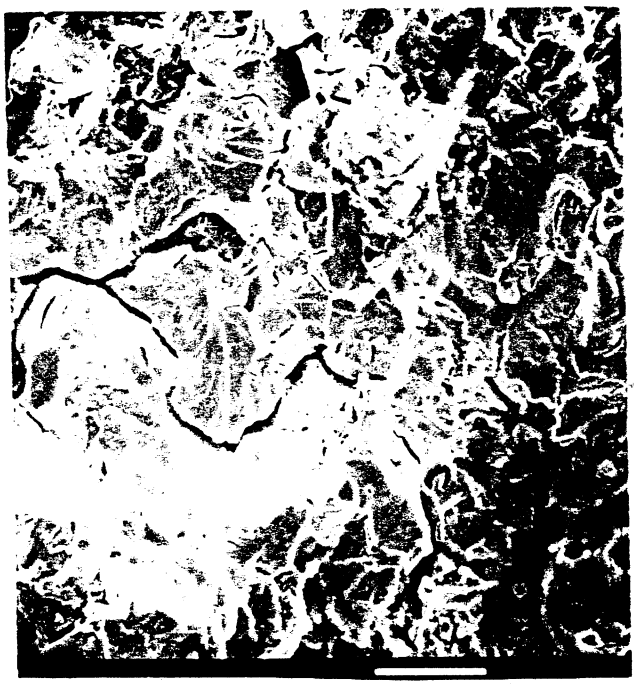

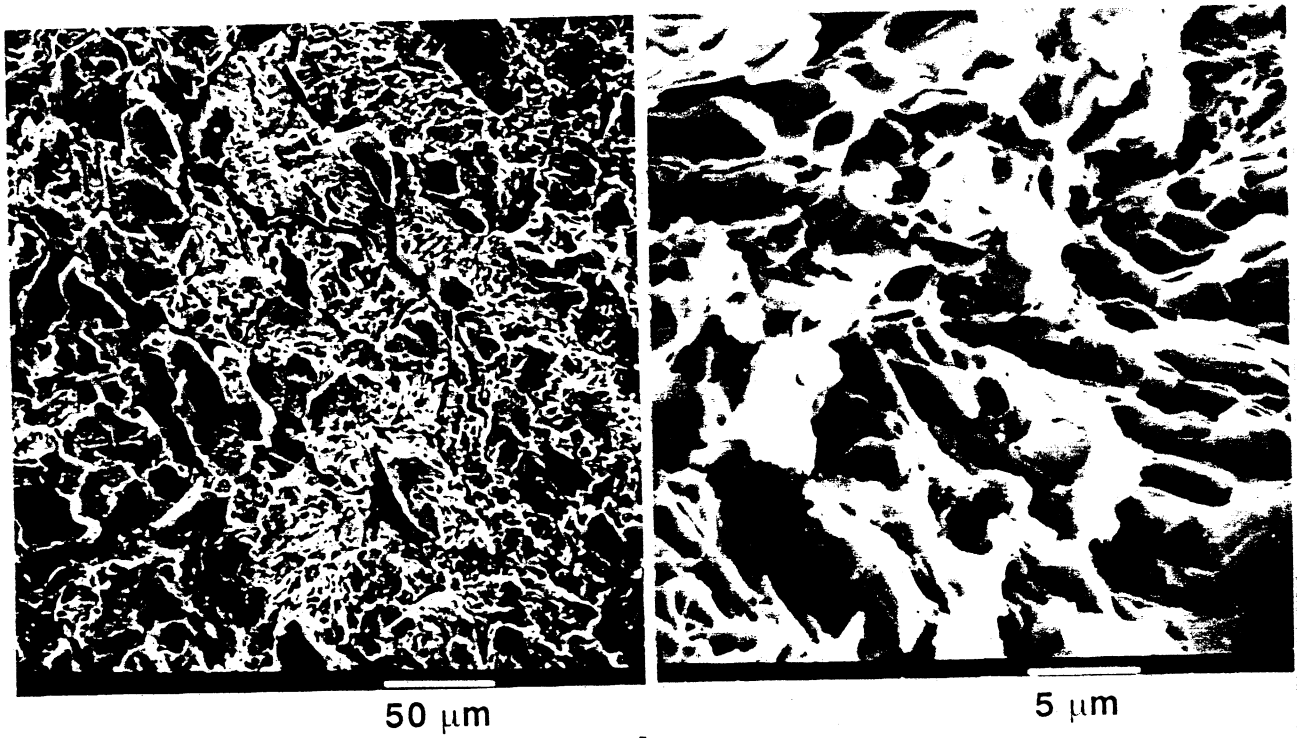

Figure 7. Effect of impact pressure on morphology of spall fracture; (a) P = 10 GPa; (b) P = 15 GPa (Courtesy of A. K. Zurek).

The ductile response of metals involves considerable plastic deformation; Figure 8(a) shows a transmission electron micrograph of a void in copper. It is surrounded by a large dislocation density evidenced by the dark region surrounding the void edges. This plastic deformation is necessary for void growth and is an intrinsic component of the plasticity models described in Section 2.1. Slip is also evident in Figure 8(b), which shows an intergranular void and the dislocation activity associated with its growth. The nucleation of voids in copper is dependent on microstructural scale parameters. If the grain size is small (Fig. 9(a)) ,the nucleation occurs homogeneously throughout the material. For large grain sizes, nucleation occurs primarily along the grain boundaries, yielding the characteristic morphology of Figure 9(b). The section through a copper specimen subjected to a tensile pulse of 3 GPa is shown in Figure 10. The right-hand-side of the figure shows the etched microstructures The nucleation, growth, and coalescence of voids at grain boundaries is obvious. Kanel et al [61] showed that the spall strength of monocrystalline copper was higher than that of pollycrystalline copper. This is contrary to their quasi-static properties and an indication that the threshold stress for grain boundary nucleation is lower than for homogeneous nucleation. These results show that the morphology of the fracture is determined by the density and spatial distribution of nucleation sites. Another clear example of a material with preferential nucleation sites at grain boundaries is shown in Figure 11. This Fe - 30 Ni alloy contains a grain-boundary precipitate (brittle carbide) which gives origin to debonding without appreciable plastic deformation.

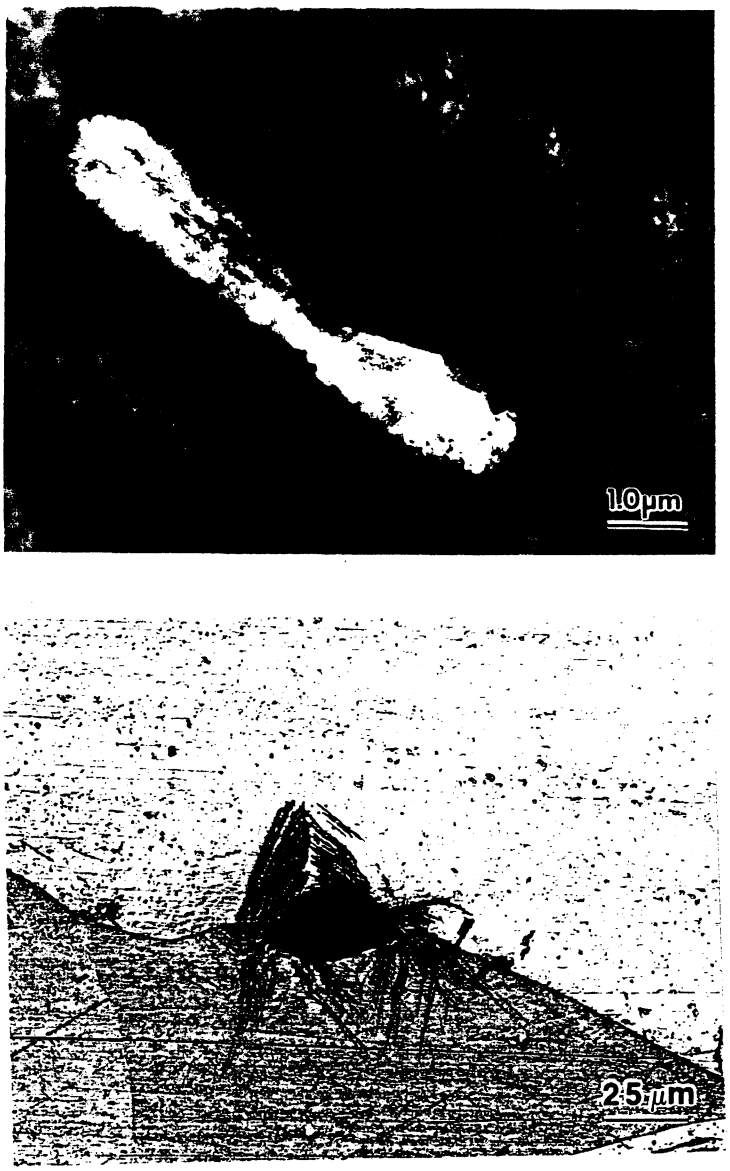

Figure 8. Voids in copper; (a) peanut-shaped void viewed by high-voltage (1MeV) transmission electron microscopy (from S. Christy, H.-r. Pak, and M. A. Meyers [60]); (b) grain boundary void with associated slip traces.

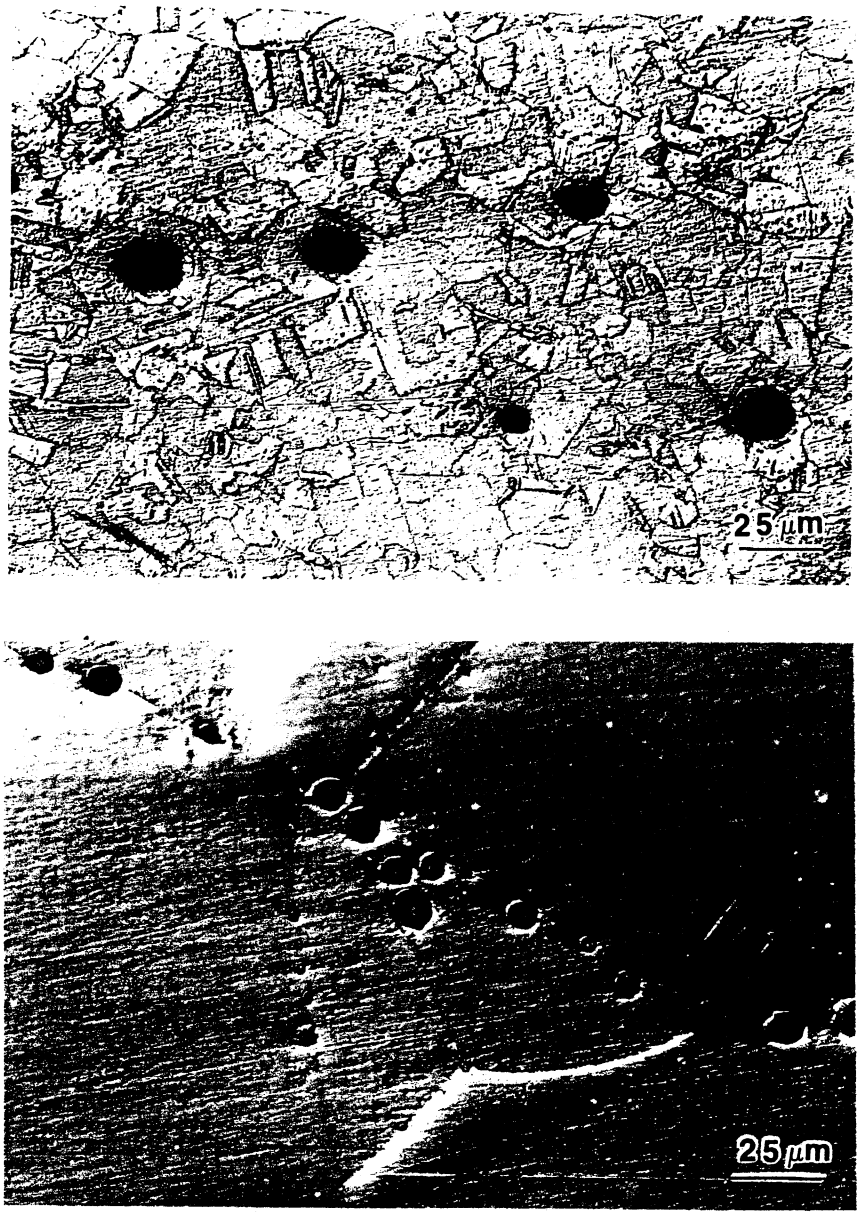

Figure 9. Effect of grain size on void distribution in copper; (a) specimen with G.S. = 20μm; (b) specimen with G.S. = 250 μm.

The morphology and breakup of voids in a dynamic tension region can lead to interesting morphologies, and one of them is shown in Figure 12(a). The voids appear to circle a region, that therefore undergoes a rotation. Benson[62] also obtained these "void sheets" ,that comprise boundaries for the domain. The evolution of one such a void agglomeration is shown in Fig 12(b). This is the result of a hydrocode computation for AISI 4340 steel.

3. DYNAMIC FAILURE IN SHEAR

3.1 Mechanical Modeling

We emphasize again that a number of excellent reviews are available in the literature. The book by Bai and Dodd[10], review articles by Rogers[63], Stelly[64] and Dormeval[65], and the proceedings of a 1992 symposium on shear instabilities[66] contain a significant amount of information.

Clifton[67], Bai[68], and Molinari and Clifton[69] introduced analyses of shear instabilities that used the perturbation method together with the conservation equations. These analyses enable the

prediction of the effect of perturbations on the onset of shear-band formation and provide a guideline to the prediction of the the evolution of a shear band. Clifton[67] improved the simplified criterion for instability proposed in the 40's:

$$\frac{d\tau}{d\gamma} = 0$$

Using an initial perturbation in temperature with wavenumber ξ,

$$\left[\frac{1}{\tau}\left(\frac{d\tau}{d\gamma}\right) + \frac{\alpha}{\rho C}\left(\frac{d\tau}{dT}\right)\right] m\dot{\gamma} + \frac{\lambda\xi^2}{\rho C} \neq 0$$

Figure 10 Cross-section of copper specimen impacted by planar/parallel flyer plate, generating pressure of 3.5 GPa; (a) unetched specimen; (b) etched specimen.

m is the strain rate sensitivity, ρ the density, C the heat capacity, α the heat-to-work conversion factor, λ the heat conductivity. The expression derived by Bai[68] is similar. Fressengeas and

Molinari[70] introduced a new perturbation method, called relative perturbation method, which accounted for the non-steadiness of plastic flow. Leroy and Molinari[71,72] extended the analysis of shear instabilities by using a two-dimensional bifurcation method. They obtained variation in shear along the band and a patterning behavior.

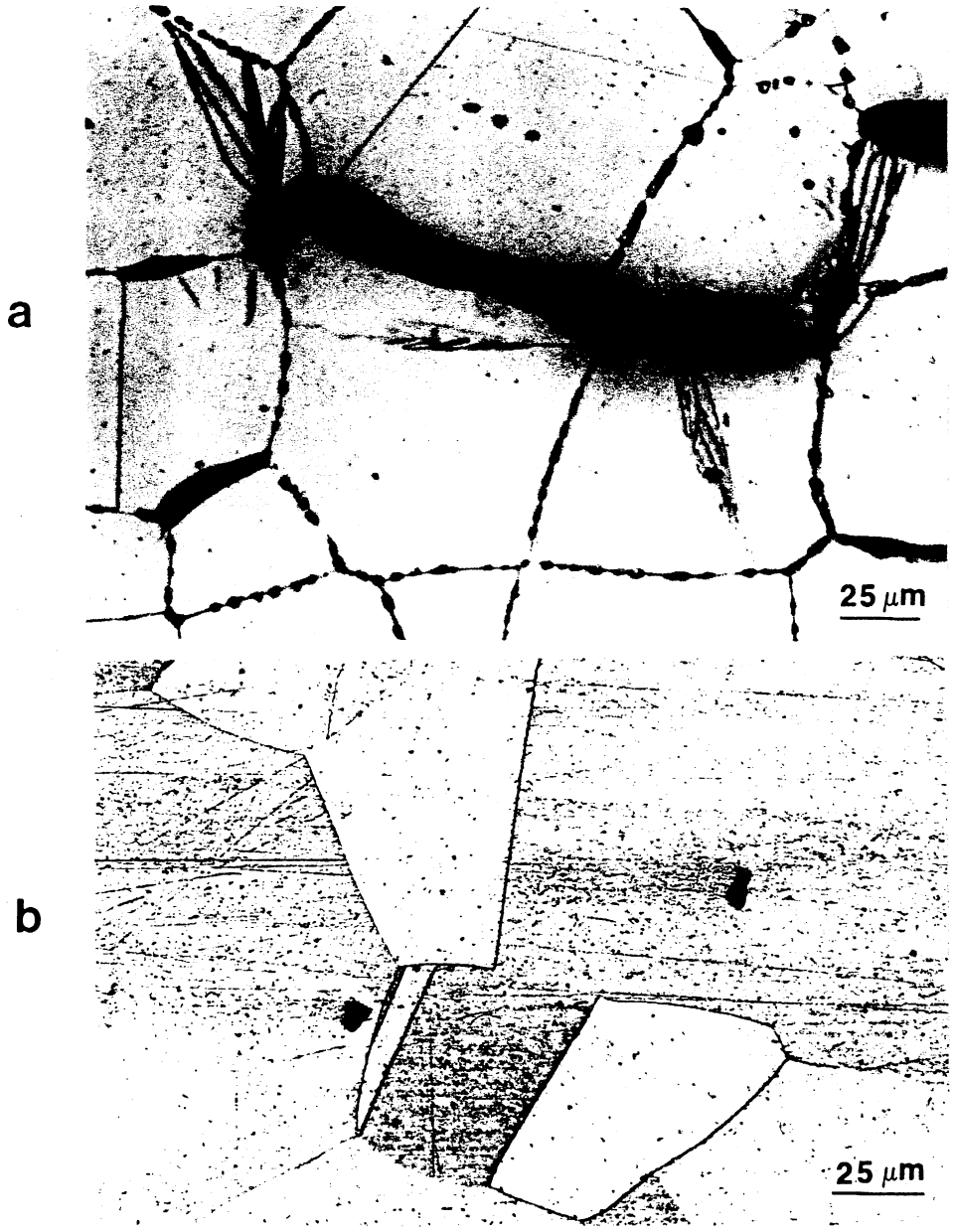

Figure 11 Incipient spalling in (a) Fe-30 Ni alloy, creating grain-boundary separation; (b) Cu, forming voids with facets.

One-dimensional models of shear bands have the limitation that the shear strain is constant along the length of the band. This is not a true realistic representation of shear bands which exhobit a front, such as a Mode II or Mode III crack, and shear strains that vary along the length of the band. This aspect was treated by Kuriyama and Meyers[73], who treated the shear band as having an extremity. They showed that the advance of a shear band proceeded by the softening of the material ahead of the tip of the band. Grady[74] developed a simplified two-dimensionalmodel for the shear band which contained a process zone. In analogy with fracture mechanics, they developed an expression for the shear-band toughness, K_s, as:

$$K_s = \sqrt{2G\Gamma_s}$$

a

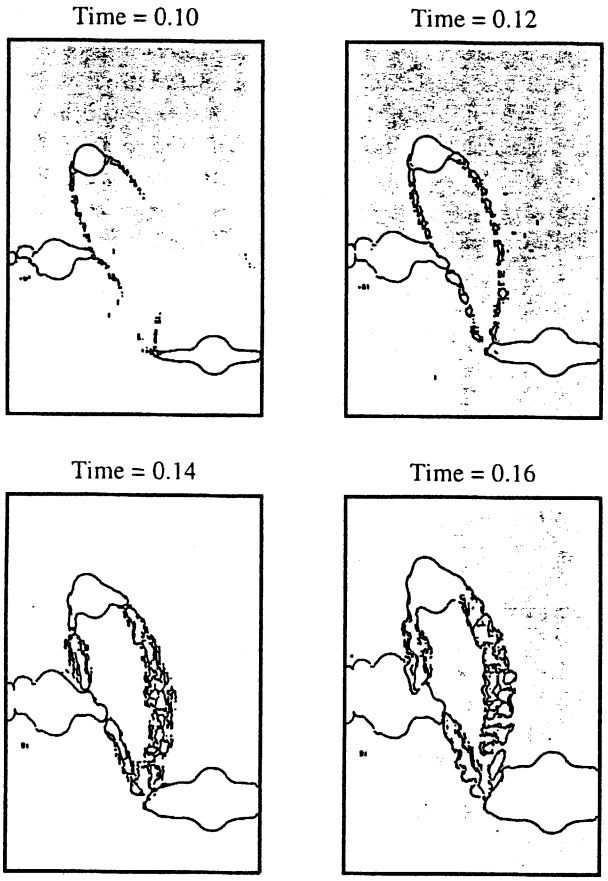

b

Figure 12 Void sheets forming circular features in spall region; (a) microstructural observation in copper; (b) hydrocode computation by D. J. Benson[62] Fig. 16.

G is the elastic shear modulus and Γ_s is the shear-band dissipation energy. This shear-band dissipation energy varies over a wide range, from 15 kJ/m^2 for uranium to 800 kJ/m^2 for copper.

3. 2 Microstructural Aspects

At the microstrutural level, the material is not a homogeneous continuum. The initiation of shear localization is a critical event, which can be triggered either by external, geometrical factors, or internal, microstructural factors. External initiation sites are regions of stress and strain concentration; microstructural sites are regions which undergo localized softening by some mechanism. Figure 13 shows in a schematic fashion, a number of these mechanisms. Possible microstructural initiation sites are fractured second phase particles (Fig. 13(c)), dislocation pile-ups being released as an avalanche (Fig. 13(d)), geometrical softening resulting from the rotation of atomic planes towards orientations with a lower Schmid factor, and preferential slip paths produced by martensite transformation and twinning. Armstrong et al[75] performed calculations that indicate that the heat generated in a pile-up release is sufficient to initiate a shear band. Another very interesting mechanism was advanced by Weertman and Hecker[76]. They proposed that local dislocation reorganization produced elongated dislocation-free regions which were initial shear bands. Meyers et al[77] made observations of a similar nature on shock-loaded nickel subjected to subsequent tension localized regions (shaped like an oblete spheroid), virtually dislocation-free, were produced from the densely deformed material, leading to shear failure by a softening mechanism.

Adiabatic shear bands are the favorate sites for failure, either by ductile void nucleation, growth, and coalescence, or by cracking. The material within the shear band is heated to a high temperature and, therefore, has a lower flow stress than the surrounding matrix. Thus, tensile stresses will open voids at the shear band. Alternatively, after cooling the material in the shear band can be harder and more brittle than the surrounding matrix. A number of examples of failure initiation at the shear bands are described by Grebe et al[78], Wittman et al[79], Meyers and Wittman[80], Beatty et al[81], and Stelly et al[82]. Figure 14 shows the formation of cracks and voids for four different alloys.

The microstructural evolution inside the shear band has been actively studied in the past 10 years, and it was independently discovered by Stelly and Dormeval[64] and Meyers and Pak[83] that the structure inside the shear band of titanium consisted of fine (less than 1 μm) recrystallized grains. Figure 15 shows these recrystallized grains for two experimental conditions. Since 1986, a number of investigators have observed recrystallized structures inside shear bands. Of particular interest are armor steels, and Meunier et al[84], and Beatty et al[81] have found strikingly analogous results: the material within the shear band consisted of nanosize grains ($\sim$ 50 nm). Figure 8 of Meunier et al[84], and Figure 10 of Beatty et al[81] are almost identical.

The importance of dynamic recrystallization in shear-band formation indicates that the critical event governing localization is the attainment of the recrystallization temperature. Thus, the material can exhibite unstable behavior, i.e., a negative slope in the true stress - true strain curve, without shear band formation. Meyers et al[85] observed this behavior for titanium and the results are shown in Figure 16. This figure shows the temperature as a function of strain for plastic deformation at 10^4 s^{-1}. Instability is reached much earlier than localization (clear shear-band formation). Similar results were found for tantalum by Chen et al[86]. The stress - strain curve shown in Figure 17(a), for 3,500 s^{-1}, decreases steadily from e = 0.1 to e = 0.7, when the test was interrupted. This softening is due to the effect of temperature on thermally-activated dislocation motion. The cross-section of the resulting specimen, shown in Figure 17(b) does not show any shear band. Localization was prevented by the temperature, which does not reach a sufficiently high level for recrystallization. The incorporation of constitutive equations which incorporate a flow stress drop due to dynamic recrystallization should help the modellers to create more realistic representations. Andrade et al[87] proposed a modified Johnson-Cook equation with a flow stress discontinuity.

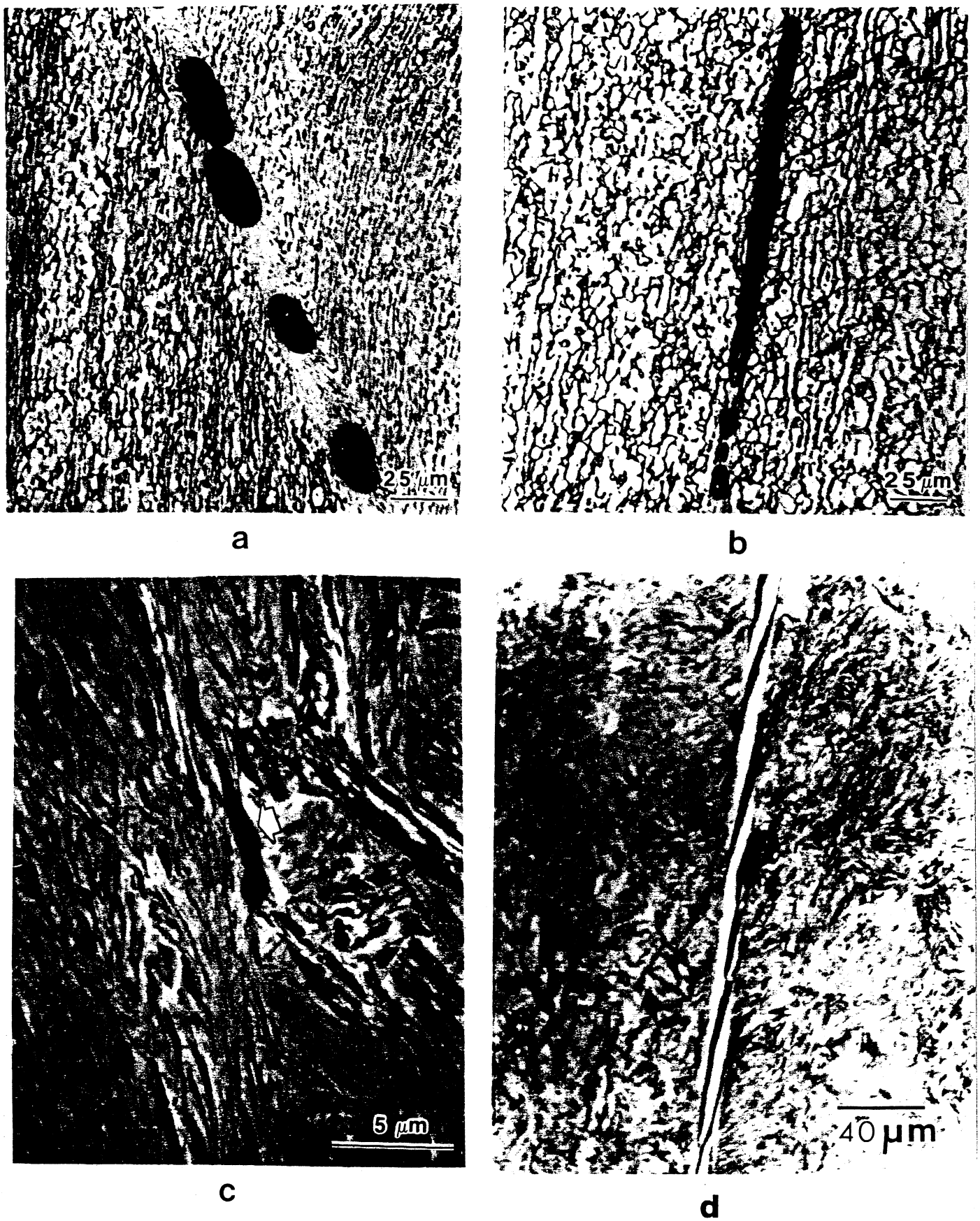

Figure 14 Crack and void formation along shear bands; (a) Ti; (b) Ti-Al-V alloy; (c) AISI1080, and (d) AISI 4340 alloy.

a

b

Figure 15 Recrystallyzed structure with grain diameters of 0.1 - 0.3 μm observed in shear band in titanium (a) From M.A. Meyers and H. r. Pak[82]; (b) From M. A. Meyers, G. Subhash, B. Kad, and L. Prasad[85].

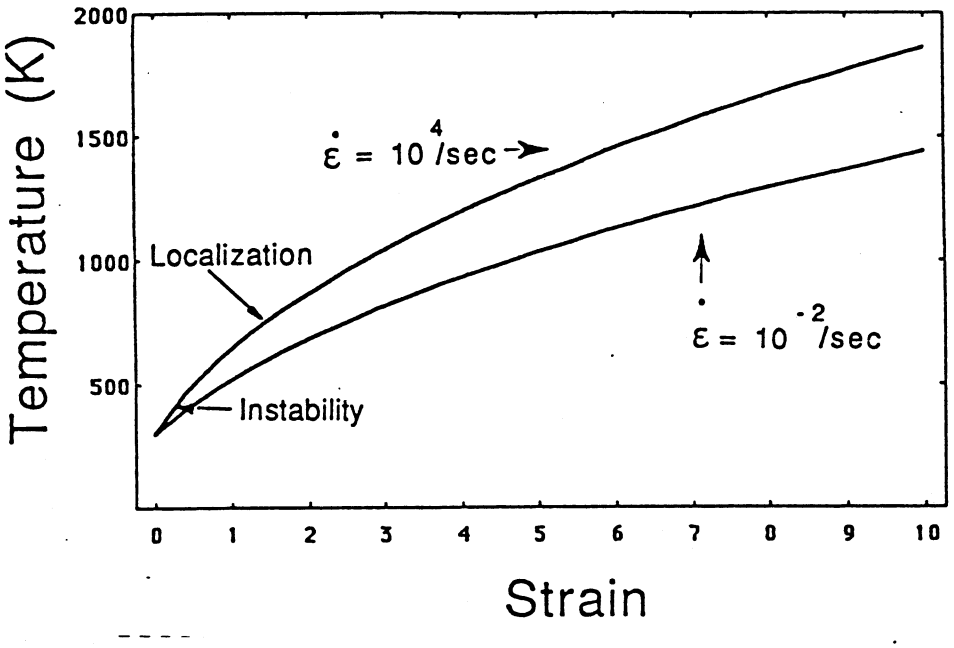

Figure 16 Temperature versus plastic strain for titanium; instability and localization temperature are indicated (From M. A. Meyers, G. Subhash, B. Kad, and L. Prasad[82].)

4. DYNAMIC FAILURE IN COMPRESSION

Whereas ductile metals can undergo large compressive strain without failure, in brittle materials (ceramics, rocks, intermetallic compounds, and brittle metals such as cast iron) flaws are generated under compressive stresses. It should be clarified that the remote compressive tractions cause, by virtue of microstructural inhomogeneities, localized regions of tension which on their turn, lead to crack initiation. Thus, microstructural effects are responsible for cracking under compression. Examples of microstructural inhomogeneities that can nucleate cracks under compression are:

- Voids, around which tensile stresses are generated by compression. These voids can have all kinds of shapes , but spheres and ellipsoids are idealized configurations which lend themselves to mathematical analyses predicting localized regions of tension.
- Grain boundaries between grains in materials having elastic anisotropy in such a manner that elastic incompatibity stresses are generated.
- Brittle grain-boundary phases which may fracture under shear resulting from compression. An example is the glassy grain-boundary phase in commercial alumina. Ceramics often contain these phases, which are due to the sintering agents that are added to material to facilitate densification during processing.
- Second-phase particles which may have different compressibilities than the matrix, leading to crack nucleation at the interface.
- Destruction of coherency between the matrix and second phases due to differences of elastic properties.

Figure 18 shows the three principal mechanisms of compressive failure in a schematic fashion. Spherical voids lead tensile stresses when loaded in compression. This problem was first solved analytically by Goodier[88] and the maximum normal tensile stress is equal to (for uniaxial stress loading)

$$\sigma^{0}_{\theta\theta} = -\frac{3}{2}\frac{(1+5\nu)}{(7-5\nu)}\sigma_1 \approx -\frac{1}{2}\sigma_1$$

σ_1 is the compressive traction. When lateral confinement is incorporated, the expression has to be modified. A generalization of the spherical void is the elliptical void, which represents a flaw of a more general shape. This was, apparently, first treated by Griffith, and analytical solutions are obtained by Brace and Bombolakis[90], Adams and Sines[91], Horii and Nemat-Nasser[92], and Ashby and Hallam[93]. Figure 18(b) shows this configuration. If ψ is the angle of the flaw plane with the compressive axis, and μ is the friction coefficient of the walls of the flaw, the maximum stress-intensity factor at the tip of flaw can be expressed as[93]:

$$K_I = -\sigma_1\left(\frac{\pi a}{3}\right)^{1/2}\left[\left(1-\frac{\sigma_3}{\sigma_1}\right)\left(1+\mu^2\right)^{1/2}+\left(1+\frac{\sigma_3}{\sigma_1}\right)\mu\right]$$

σ_1 is the compressive traction and σ_3 is the lateral confinement. This occurs for the orientation

$$\psi = \frac{1}{2}\tan^{-1}\left(1/\mu\right)$$

a

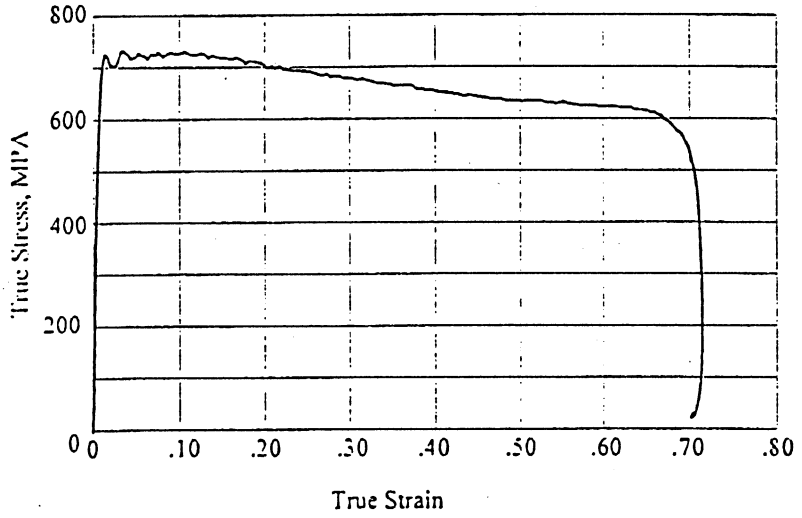

b

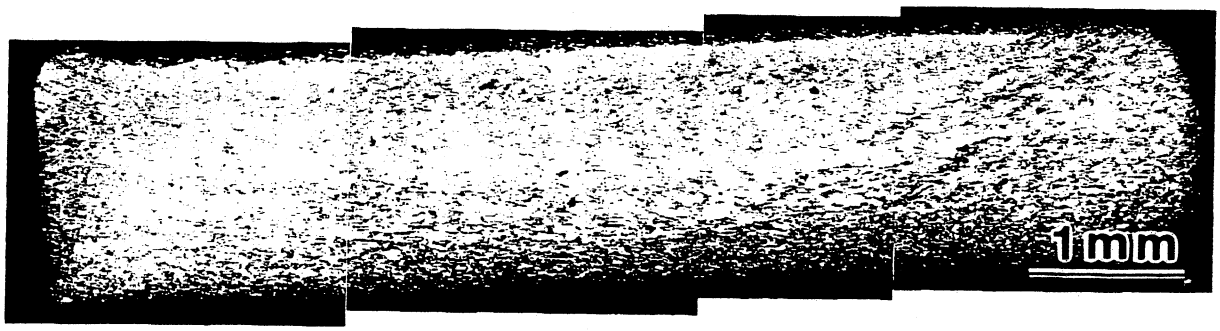

Figure 17 (a) True-stress true-strain curve for tantalum at 3,500 s^{-1}, and (b) cross-section of specimen, showing absence of localization (From M.A. Meyers, F. Marquis, Y. J. Chen, and J. B. Isaacs[86]).

Nemat-Nasser and Deng[95] considered an array of wing cracks (shown in fig. 18(b)) in a ceramic subjected to compression. They obtained closed-form solutions for the ceramic, for dynamically growing and interacting cracks. They applied a form of the above equation to these cracks, varying both the stress state (uniaxial stress and strain) and strain rate, $\dot{\varepsilon}$. Lateral confinement (represented by uniaxial strain) is very important and increases the compressive

strength. The microstructural parameters were introduced through the crack length, 2a, and spacing, 2w. The failure stress, which was dependent on a, w, $\dot{\varepsilon}$, and stress state, was observed to increase significantly in the 10^4 - 10^6 s^{-1} range.

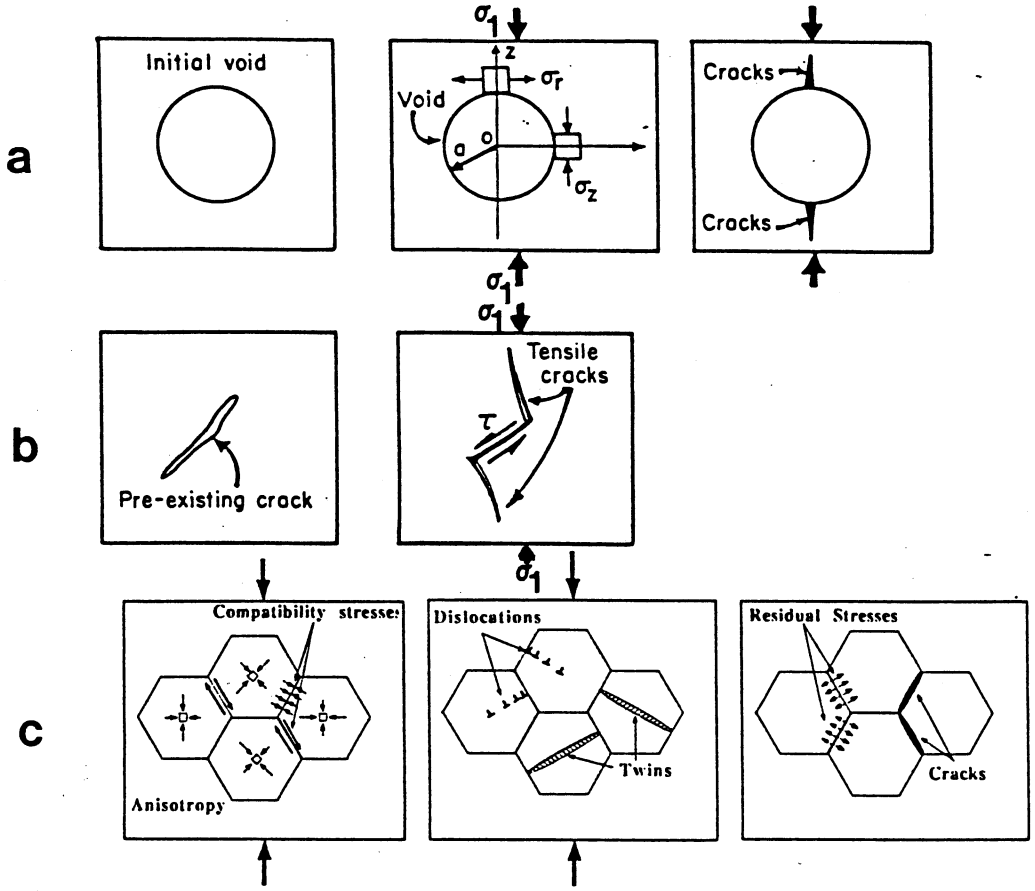

Figure 18 Different mechanisms for crack formation in compressive loading of brittle materials. (From M. A. Meyers [1],).

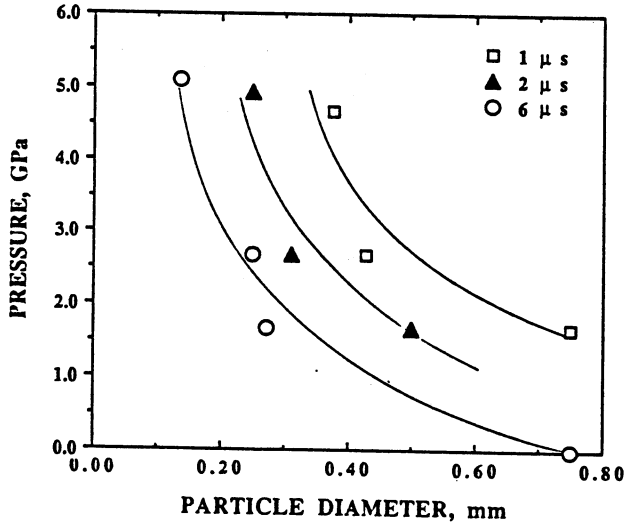

Figure 19 Effect of pressure and pulse duration on fragmentation of quartz monzonite loaded in compression.

The third mechanism of flaw formation due to compression is shown in Figure 18(c). It is due to the anisotropy of elastic properties of grains, and to generation of dislocations and deformation twins, generated in loading. Internal stress gradients are generated by these effects. These stresses can generate cracks, on unloading, when the stress concentrations act on the grain boundaries. Lankford[96] has shown that flaws can appear in ceramics when loaded to a fraction of the fracture stress. Louro and Meyers[53] have shown that dislocation activity was present in a small fraction of the grains in alumina, when loaded below the HEL.

A dislocation pile-up can generate high tensile stress at a grain boundary. Thus, when the material in unloaded, these tensile stresses can generate grain-boundary fracture. The normal stress parallel to the Burgers vector of a dislocation is:

$$\sigma_{11} = -\frac{Gb}{2\pi(1-\nu)}\frac{x_2\left(3x_1^2 + x_2^2\right)}{\left(x_1^2 + x_2^2\right)^2}$$

A pile-up of n dislocations generates a stress, as shown by Eshelby [98] and Stroh[97], of $n\sigma_{11}$. This superdislocation is situated at 1/4 from the pile-up head. If the grain size is D, the distance x_1 is D/8 and the tensile stress acting on the boundary is:

$$\sigma_t = \frac{16nGb}{\pi(1-\nu)D^2}$$

x_2 was assumed to be equal to - x_1. For alumina, a typical ceramic, and D = 10 μm,(x_1=1.2 μm); thus the tensile stress is approximately 80n GPa.

Sun and Field[94] carried out experiments in alumina by impacting targets with spherical projectiles and were able to correlate their results with the mechansms discussed in this section. Experiments carried out by Aimone, Meyers, and Mojtabai[99] on a rock (quartz monzonite) subjected to compressive pulses of varying amplitudes and durations revealed that the fragmentation was a function of both the amplitude of the compressive pulses and on the duration. Thus, the kinetics of crack nucleation and growth during compression is instrumental in establishing the final fregmentation. Figure 19 shows these results. As the pulse duration is increased, for a constant pressure, the fragment size are decreased. These are "apparent" fragment sizes, measured from flaw surface area per unit volume, S_v, and converted into an "apparent" damage size, D, by:

$$D = \frac{6}{S_v}$$

There have been recent reports of a failure wave propagating in glass and ceramics when impacted at high velocities. These reports by Kanel et al[100], and Brar and Bless[101], have not uncontrovertibly confirmed. Experimental results by Senf and Strassburger[102] seem to indicate that this failure wave is simply the activation of flaws by either the longitudinal or shear wave.

Johnson and Holmquist[103] and Cosculluela[56] have developed a constitutive model which describe brittle materials under compressive loading. The failure of composites under dynamic compressive loading has been discussed by Harding[104]. Composites have a complex response which was not treated in this article due to lack of space.

5. SUMMARY AND CONCLUSIONS

The observations reported in this article as well as extensive information in the literature indicate that microstructural aspects are of utmost importance in the dynamic failure of materials.

The mechanical models have progressed to the point where they incorporate the most important physical phenomena in dynamic failure. Advanced computational methods (especially, finite elements, finite differences, and molecular dynamics codes) can capture the complex

phenomenology of dynamic failure. In parallel, analytical, closed-form solutions have been developed for a large number of loading situations and microstructural configurations.

Dynamic failure can be divided into three classes:

1) Dynamic failure by tension; spalling (uniaxial strain state) and uniaxial stress state.
2) Dynaimc failure by shear; shear instability is the precursor to this failure mode.
3) Dynamic failure by compression; ceramics, rocks and brittle metals (cast iron, intermetallic compounds) are especially prone to failure under compressive loading.

We summarize below the most important microstructural effects for these three classes of failure. All microstructural variables play a role in the dynamic failure of materials. The most important variables are:

- grain size
- presence, density, morphology, and size and distribution of second-phase particles
- texture (not mentioned in this chapter)
- impurity atoms and their distribution (e.g., segregation at grain boundaries)
- crystallographic structure (which can be changed by heat treatment, e.g., quenching of steel)
- pre-strain (e.g., annealed vs. shock-hardened material)
- intergranular phases (e.g., glassy phase at grain boundaries of ceramic)
- voids (e.g., porosity in the ceramics) and microcracks.

ACKNOWLEDGMENTS

This research was made possible through the support of the U. S. Army Research Office URI Program, the National Science Foundation Grant MSS - 9021671, and the Center for Explosives Technology Research, New Mexico Tech. Collaborations and discussions with U. R. Andrade, D. J. Benson, H. C. Chen, Y. J. Chen, S. Christy, H. A. Grebe, J. Isaacs, B. Kad, L. H. L. Louro, F. Marquis, L. W. Meyer, S. Nemat-Nasser, V. Nesterenko, N. N. Thadhani, K. S. Vecchio, and A. Zurek are greatly appreciated.

REFERENCES

1. Meyers, M. A., "Dynamic Behavior of Materials", J. Wiley, NY, 1994.
2. Rinehart, J. S., and Pearson, J., "Behavior of Metals under Impulsive Loads", ASM, Dover, NY, 1964.
3. Kolsky, H., "Stress Waves in Solids", Dover, NY, 1963.
4. Goldsmith, W., "Impact", E. Arnold, UK, 1960.
5. Johnson, W., "Impact Strength of Materials", E. Arnold, UK 1972.
6. Freund, L. P., "Dynamic Fracture Mechanics", Cambridge U. P., UK, 1990.
7. Asay, J. R., and Shahinpoor, M.,eds.,"High-Pressure Shock Compression of Solids",Springer, NY,1993.
8. Davison, L., Grady, D., and Shahinpoor, M.,eds., "Dynamic Fracture and Fragmentation', Springer, NY,1994.
9. Ahmadeyev, N. K., "The Dynamic Failure of Solids",, USSR Acad. of Sci., FSU, 1988.
10. Bai, Y., and Dodd, B., "Adiabatic Shear Localization", Pergamon, Oxford, 1992.
11. Bushman, A. V., Kanel, G. I., Ni, A. L., and Fortov, V. E., "Intense Dynamic Loading of condensed Matter", Taylor & Frances, Bristol, PA 1992.
12. Graham, R. A., "Solids Under High-Pressure Shock Compression", Springer, NY, 1993.
13. Zukas, J. A., ed., "High Velocity Impact Dynamics", J. Wiley, NY, 1991.
14. Curran, D. R., Seaman, L., and Shockey, D. A., "Dynamic Failure of Solids", Phys. Rep. 147 (1987) 253.
15. Meyers, M. A., and Aimone, C. T., Prog. Matls. Sci. 28 (1983) 1.
16 Zurek, A. K., and Meyers, M. A., source cited in ref. 7.
17. Mott, N. F. ,Engineering,165,(1948),
18. Yoffé, H., Phil Mag. 42 (1951) 739.
19. Broberg, K. B., Arch. für Physik, 18 (1960) 159.
20. Craggs, J. W., J. Mech. Phys. Sol. 8 (1960) 66.

21. Baker, B. R., J. Appl. Mech., 29 (1962) 449.
22. Achenbach, J. D., "Dynamic Effects in Brittle Fracture", in Mechanics Today, ed. S. Nemat-Nasser, Vol. 1, Pergamon, 1974, p. 1.
23. Freund, L. B., J. Mech. Phys. Sol., 20 (1972) 129.
24. Freund, L. B., J. Mech. Phys. Sol., 20 (1972) 141.
26. Freund, L. B., J. Mech. Phys. Sol., 21 (1973) 47.
24. Freund, L. B., Int. J. Eng. Sci., 12 (1974) 179.
27. Freund, L. B., "The Analysis of Elastic-dynamic Crack Tip Stress Fields", in Mechanics Today, ed. S. Nemat-Nasser, Vol. 3, Pergamon Press, 1976, p. 55.
28. Freund, L. B., "Dynamic Fracture Mechanics", Cambridge U. Press, 1990.
29. Congleton, J., "Practical Applications of Crack-Branching Measurements", in "Dynamic Crack Propagation", ed. G. S. Sih, Noordhof, Leyden, 1973, p. 427.
30. Sih, G. C., "Dynamic Aspects of Crack Propagation", in "Inelastic Behavior of Solids", eds. M. F. Kanninen, W. F. Adler, A. R. Rosenfield, and R. I. Jaffee, McGraw Hill, NY, 1970, p. 607.
31. Ravi-Chandar,G., and Knauss,W. G.,Intl. J. Fract., 26(1984)141.
32 Winkler, S., Shockey, D. A., and Curran, D. R., Int. J. Fract. Mech. 6 (1970) 151.
33. McClintock, F. A., J. Appl. Mech. 35 (1968) 363.
34. McClintock, F. A., Int. J. Fract. Mech., 4 (1968) 101.
35. Rice, J. R., and Tracey, D. M., J. Mech. Phys. Sol., 17 (1969) 201.
36. Glennie, E. B., J. Mech. Phys. Sol., 20 (1972) 415.
37 Rice, J. R., and Johnson, M. A., in "Inelastic Behavior of Solids", ed. M. F. Kanninen, W. F. Adler, A. R. Rosenfield, and R. I., Jaffee, McGraw-Hill, NY, 1970, p. 641.
38. McMeeking, R. M., Trans. ASME, J. Eng. and Techn. 99 (1977) 290.
39. Gurson, A. L., J. Eng. Mater. Tech., 99 (1977) 2.
40. Fyfe, I. M., in" Material Behavior Under High Stress and Ultrahigh and Ultrahigh Loading Rates", eds. J. Mescall and V. Weiss, Plenm, NY,1983, p. 309.
41. Johnson, J. N., J. Appl. Phys., 52 (1981) 2812.
42. Caroll, M. M., and Holt, A.C., J. Appl. Phys., 43 (1972) 1626.
43. Davison, L., and Stevens, A.L., J. Appl. Phys., 44 (1973) 688.
44. Mott, N. F., Proc. Roy. Soc. 300(1947) 300.
45. Grady, D.E., and Kipp, M.E., Intl. J. Rock Mech. Min. Sci. 17(1989) 147.
46. Grady, D. E., J. Appl. Phys., 55 (1982)322.
47. Ke, F., Bai, Y., and Xia, M., Science in China 33 (1990) 1447.
48. Bai, Y., Ke, F., and Xia, M., Acta Mech. Sin., 7 (1991) 59.
49. Xia, M., Ke, F., Lu, Y., and Bai, Y., Science in China, 34 (1991), 579.
50. Louro, L. H. L., and Meyers, M. A., J. de Phys., 49, 3-333 (1988) (Colloque - 3).
51. Louro, L. H. L., and Meyers, M. A., in " Shock Waves in Condensed Matter - 1989 ", eds. S. C. Schmidt, J. N. Johnson, and L. W. Davidson, North Holland, (1990), 465.
52. Field, J. E., " Investigation of the Impact Performance of Various Glass and Ceramic Systems ", Final Report, Contract D A, JA45-85-C-0021, Cavendish Laboratory, Cambridge, England, 1985.
53. Louro, L.H.L., and Meyers, M.A., J. Matls. Sci., 24 (1989) 971.
54. Longy, F. and Cagnoux, J. , J. Am. Cer. Soc. 72 (1989) 971.
55. Cosculluela, A., Cagnoux, J., and Collombet, F., J. de Physique, IV, Coll. C3 (1991). C3-109.
56. Cosculluela, A.,Thesis,U. of Bordeaux I, 1992.
57. Zurek, A.K., and Follansbee, P.S., in "Shock Compression of Condensed Matter-1989". eds. S.C. Schmidt, J.N. Johnson, and L.W. Davison, North Holland, 1990, p.433.
58. Ivanov, A.G., and Novikov, S.A., J. Exp. Theor. Phys. (USSR), 40 (1961) 1880.
59. Zurek, A.K. Follansbee, P.S., and Hack, J., Met. Trans. 21A (1990) 431.
60. Christy, S., Pak, H.-r,., and Meyers, M.A. in "Metallurgical Applications of Shock-Wave and High-Strain Rate Phenomena, eds. L. E. Murr, K. P. Staudhammer,, and M. A. Meyers, , M. Dekker, NY, 1986, p. 835.
61. Kanel, G.I., Rasorenov, S.V., and Fortov, V.E., in "Shock-Wave and High-Strain-Rate Phenomena in Materials, eds. Meyers, M.A., Murr, L.E., and Staudhammer, K.P., M. Dekker, 1992, p.775.
62. Benson, D. J., J. Mech. Phys. Sol., 41 (1993) 1285.
63. Rogers, H.C., Ann. Rev. Mat. Sci. 9 (1979) 283.
64. Stelly, M., and Dormeval, R., in "Metallurgical Applications of Shock-Wave and High-Strain-Rate Phenomena", eds. L.E. Murr, K. P. Staudhammer, and M.A. Meyers., M. Dekker, NY, 1986, p. 607.

65. Dormeval, R. in "Impact Loading and Dynamic Impact in Behavior of Materials; eds. C.Y.. Chiem, H.-D. Kunze, and L. W. Meyer, Informationsg., D.G.M., 1988, p.43
66. Armstrong, R.W., Batra, R., Meyers, M.A., and Wright, T.W., eds., Mech. of Matls., 17(1994) 83-328.
67. Clifton, R. J., Material Response to Ultra-High Loading Rates, Report No. NMAB-356, Natl,. Matls. Advs. Board, NAS, Washington, Chapter 8 (1979).
68. Bai, Y., in "Shock Waves and High-Strain-Rate Phenomena in Metals: Concepts and Applications, eds. M.A. Meyers and L.E. Murr, Plenum, NY, (1981) 277.
69. Molinari, A., and Clifton, R.J., Comptes Rendus, Acad. Sci. Paris, 296(1983)1.
70. Fressengeas, C., and Molinari, A., J. Mech. Phys. Sol., 35 (1987) 185.
71. Le Roy, Y.M., and Molinari, A., L. Mech. Phys. Sol., 41 (1993) 631.
72. Molinari, A., and LeRoy, Y.M., C.R. Acad. Sci. Paris, 313 (1991) 7.
73. Kuriyama, S., and Meyers, M.A., Met. Trans., 17A (1986) 443.
74. Grady, D.E., Mech. of Matls., 17(1994)289.
75. Armstrong, R.W., Coffey, C.S., Elban, W.L., Acta Met. 30 (1982) 2111.
76. Weertman, J., and Hecker, S.S., Mech. of Matls. 2 (1983) 89.
77. Meyers, M.A., Hsu, K.-C., and Couch-Robino, K., Mater. Sci. Eng. 59 (1983) 235.
78. Grebe, H.A., Pak, H.-r., and Meyers, M.A., Met. Trans. 16A (1985) 711.
79. Wittman, C.L., Meyers, M.A., and Pak, H.-r., Met. Trans. 21A (1990) 707.
80. Meyers, M.A., and Wittman, C.L., Met. Trans. 21A (1990) 3193.
81. Beatty, J.H., Meyer, L.W., Meyers, M.A., and Nemat-Nasser, S., in "Strain-Rate Phenomena in source cited in ref. 61, p.645.
82. Stelly, M., Le Grand, J., and Dormeval, R., in "Schock Waves and High-Strain-Rate Phenomena in Metals", eds. M.A. Meyers and L.E. Murr, Plenum, NY, 1981, p.113.
83. Meyers, M. A., and Pak, H. -r., Acta Met. 34(1986), 2493.
84. Meunier,Y., Roux, and Moueaud, J., in source cited in ref. 61, p. 637.
85. Meyers, M. A., Subhash, G., Kad, B. K., and Prasad, L., Mech. of Matls, 17(1994), 175.
86 Chen, Y. J., Marquis, F., Meyers, M. A., and Isaacs, J. B., Met. Trans., to be submitted, (1994).
87. Andrade, U. R., Meyers, M.A., and Chokshi, A. H., Scripta Met. et Mat., 30(1994), 933.
88. Goodier, N., J. Appl. Mech., 1(1993), 39.
89. Sammis, C. G.,and Ashby, M. F., ,Acta Met., 34(1986),511.
90. Brace, W. F., and Bombolakis, E. G., J. Geophys. Res., 68(1963), 3709.
91. Adams, M., and Sines, G., Tectonophysics, 49(1978), 97.
92. Horii, H., and Nemat-Nasser, S., Trans. Roy. Soc., London, 319(1986), 33
93. Ashby, M. F.,and Hallam,S. D., Acta Met., 34(1986), 497.
94. Sun, Q., and Field, J., Proc. Intl. Symp. On Intense Dynamic Loading and its Effects, Chengdu, China, Sechuan U. Press, 1992, p.384.
95. Nemat-Nasser, S., and Deng, H., Acta Met. Mat. et Mat., 42(1994), 1013.
96. Lankford, J. ,J. Matls. Sc., 12(1977), 791.
97. Stroh, A. N., Proc. Roy. Soc.(London), A223(1954), 404.
98. Eshelby,J. D., Frank, F. C., And Nabarro,F. R. N., Phil. Mag., 42(1951), 351.
99. Aimone, C. T., Meyers, M. A., and Mojtabai, N., in "Rock Mechanics in Productivity and Protection", eds., C. H. Dowding and M. M. Singh,AIME,1984, p.979.
100. Kanel, G.I., Rasorenov, S. V., and Fortov, V. E., in " Shock Compression of Condensed Matter ", eds. S. C. Schmidt et al, Elsevier, 1992, 451.
101. Brar, M. S., and Bless, S. J. in source cited in ref. 61, p.1041.
102. Senf, H., and Strassburger, E., Ernst-Mach Institute, private communication, (1994).
103. Johnson, G. R., and Holmquist, T. J., in source cited in ref. 61, p.1075.
104. Harding, J., in source cited in ref. 61, p.21.